EVALUATING RARE EARTH ELEMENTS AS TRACERS OF FLUVIAL PROCESSES: FINE SEDIMENT TRANSPORT AND DEPOSITION IN A SMALL STREAM

Heather Govenor[1], W. Cully Hession[2,*], Tyler A. Keys[3], C. Nathan Jones[4], Ryan D. Stewart[5], Leigh-Anne H. Krometis[6]

[1] EnSafe Inc., Memphis, Tennessee, USA.
[2] Department of Biological Systems Engineering, Virginia Tech, Blacksburg, Virginia, USA.
[3] U.S. Army Corps of Engineers, Sacramento, California, USA.
[4] Department of Biological Sciences, University of Alabama, Tuscaloosa, Alabama, USA.
[5] Department of Crop and Soil Environmental Sciences, Virginia Tech, Blacksburg, Virginia, USA.
[6] Department of Biological Systems Engineering, Virginia Tech, Blacksburg, Virginia, USA.
[*] Correspondence: chession@vt.edu.

HIGHLIGHTS

- Natural sediments labeled with rare earth elements can effectively be used as tracers for quantifying fine sediment transport and deposition.
- Two artificial floods in a small stream (100 ha watershed, 1.5 year return flow of 515 L s^{-1}) transported fine sediment 0 m to >850 m at a maximum flow rate of 55 L s^{-1}.
- Sediment deposition per unit area was greater in the channel than in the near-channel floodplain.
- Use of two distinct tracers demonstrated resuspension extent during sequential high-flow events.
- Presence of large wood in the channel was associated with reduced streamflow rate, decreased suspended sediment transport velocity, increased channel sediment deposition, and reduced near-floodplain sediment deposition.

ABSTRACT. *Effective sediment management requires an understanding of the lag time between best management practice implementation and observable changes in the target water body. To improve our understanding of sediment lag times, we tested a method to label locally sourced sediments with rare earth elements to quantify fine sediment flow-through and storage in fluvial systems. We injected sediments labeled with lanthanum and ytterbium into a small stream during two artificial flood events. During the floods, we collected and quantified suspended sediments and sediment deposition in the stream channel and floodplain at four cross-sections within our study reach. Two down-gradient (90 m and 850 m) time-integrated suspended sediment samplers evaluated total travel distance. Sediment tracer observations of particle transport distances ranged from 0 m to at least 850 m at a maximum flow rate of 55 L s^{-1} (stream 1.5 year flow was 515 L s^{-1}). Sediment deposition per unit area was greater in the channel than in the floodplain. The majority of sediment tracer mass injected into the stream entered storage within the first 69 m of the reach. Some particles that deposited following the first flood were resuspended and either transported downstream or redeposited within the study reach. Our results support the further use of rare earth elements as sediment tracers to inform water quality and sediment transport models, and to provide estimates of lag times between management actions and downstream improvements.*

Keywords. *Fine sediment, Flood, Fluvial geomorphology, Lag time, Large wood, Rare earth elements, Sediment deposition, Sediment transport, Tracer.*

Sediment imbalance is the second most common cause of freshwater river and stream impairment in the U.S. (USEPA, 2016). Excess fine sediment can fill reservoirs, interfere with navigational channels, reduce flood control capacity (Owens, 2008), and cause shifts in fish, macroinvertebrate, and periphyton communities (Waters, 1995; Wood and Armitage, 1997; Chapman et al., 2014; Govenor et al., 2017). Sediment can also convey attached contaminants and nutrients, which have associated environmental and human health impacts (Characklis et al., 2005; Owens et al., 2005). The economic impacts of sediment contamination on surface waters are considerable. In North America alone, the costs of human-induced sediment loadings into freshwater systems have been estimated at $20 billion to $50 billion annually (Miller et al., 2015).

Sediment management generally focuses on source control (USEPA, 1999), which involves limiting the loading of sediments into water bodies through treatment of or restrictions on point-source discharges and the implementation

Submitted for review on 12 October 2020 as manuscript number NRES 14358; approved for publication as a Research Article by the Natural Resources & Environmental Systems Community of ASABE on 24 February 2021.

  ISSN 2151-0032 https://doi.org/10.13031/trans.14358

of best management practices (BMPs) to limit nonpoint-source inputs. Reduced loadings are expected to translate into reductions of in-stream sediments as excess sediment is flushed from the channel during subsequent high-flow events. However, lag times between sediment loading reductions and water quality improvements in the reach or at the watershed outlet are highly variable and can extend to decades or more (Meals et al., 2010; Pizzuto et al., 2014). This temporal disconnect between restoration investments and the return of a healthy ecosystem can make it difficult to communicate to stakeholders and the general public when improvements can be expected to demonstrate a return on their investment (Martin-Ortega et al., 2017); public appreciation of ecological restoration efforts often takes time (Åberg and Tapsell, 2013). Having reliable estimates of lag times is critical to the establishment of appropriate monitoring programs and for framing realistic expectations for stakeholders regarding the timeframe for watershed improvements (CBPSTAC, 2013).

Lag times are influenced by the specific BMP implemented as well as a variety of watershed traits including drainage area, soil types, geology, topography, channel geometry, in-stream structures, climate, and precipitation (Meals et al., 2010; Hamilton, 2012; CBPSTAC, 2013). These watershed traits influence key facets of sediment cycling including suspension, transport, and storage. Previous studies of sediment fate and transport within stream channels have predominantly focused on the transport of bed particles, which is critical for understanding channel evolution (Habersack et al., 2017; Mao et al., 2017). However, an understanding of fine sediment fate and transport is necessary for predicting BMP impacts on downstream nonpoint-source pollution and aquatic ecology. While the tracking of larger-sized particles that comprise bedload can be conducted via painting of individual particles (Quinlan et al., 2015), radio transmitters (Mao et al., 2017), and magnet tags (Ferguson et al., 2017), the tracking of smaller particles within a stream system presents unique challenges.

The tracking of fine sediments falls into two main categories: sediment fingerprinting and transport or tracer studies. These techniques, in turn, can be viewed through either a Eulerian (movement of sediment past a place through time) or Lagrangian (movement of a specific particle of sediment through space and time) reference frame (Doyle and Ensign, 2009). Sediment fingerprinting, a Eulerian approach, is a technique that aims to identify landscape sources and their relative sediment loading contributions to streams. A combination of approaches is used to identify sediment sources, including natural variations in mineralogy, isotopic ratios, particle size, magnetism, bacterial signatures, and other chemical, physical, and biological characteristics (Guzmán et al., 2013; Haddadchi et al., 2013). A variety of mixing models can subsequently be applied to these data to determine sediment source contributions (Haddadchi et al., 2013). Although useful in demonstrating specific linkages between upland practices and in-stream loadings, fingerprinting does not provide a detailed spatial and temporal view of actual sediment particle fate within the stream channel.

Fluvial sediment transport or tracer studies track sediment particles within the stream channel directly and monitor suspended sediment concentrations and turbidity to quantify sediment release, transport, and fate over time (Gao, 2008; Larsen et al., 2010). Historical releases of contaminated sediments have also been interpreted as decadal sediment tracer experiments (Pizzuto, 2014). For higher-resolution tracing studies over shorter time scales, the injection of artificial fluorescent particles allows more detailed, smaller-scale evaluation of fine particle fate and transport (Drummond et al., 2017). Stable isotopes have also been identified as having potential to serve as sediment tracers within aquatic environments (Miller et al., 2015), and short-lived fallout radionuclides have been used to track lateral migration rates in meandering rivers (Black et al., 2010). Experimental approaches to sediment tracing include the use of radio-frequency identification (RFID) technology to track the movement of individual cobbles and rocks using a Lagrangian framework (Bertoni et al., 2010), and the application of rare earth elements (REEs) to upslope soils in order to track erosion and down-gradient deposition using a Eulerian approach (Polyakov et al., 2009).

Quantifying fluvial sediment transport using sediment labeled with REEs presents a novel and potentially valuable means to directly observe and quantify sediment movement, storage, and release. REEs are naturally occurring elements belonging to the lanthanide series (atomic numbers from 57 through 71). While not "rare" in terms of overall abundance, they have a low tendency to concentrate into ore deposits, resulting in limited concentrated sources (USGS, 2002). A review by Guzmán et al. (2013) indicated that while several sediment tracer studies have employed REEs, these studies have predominantly focused on hillslope erosion to track movement of sediments within plots or agricultural fields (Polyakov and Nearing, 2004; Michaelides et al., 2010; Guzmán et al., 2013; Haddadchi et al., 2013); a limited number of studies have applied this technique to receiving waters. Mahler et al. (1998) used REE-labeled clay to trace fine sediment transport during uniform flow in a small surface stream in karst geology, and Spencer et al. (2011) used REE-labeled clay to monitor fine sediment circulation and deposition within a stormwater detention pond.

The present study used two distinct REEs to track fine sediment transport and storage in a first-order stream during two distinct artificial floods (conducted one day apart and employing a distinct REE in each flood) within a Eulerian framework (Doyle and Ensign, 2009). This study demonstrates proof of concept of the work of Kreider (2012), who developed the initial concepts and demonstrated binding of REE to natural soils. Our goal was to demonstrate the potential use of REE for tracking sediment fate and transport in fluvial systems to increase our understanding of sediment lag times. Our specific objectives were to:

1. Determine if REE-labeled sediment can be used to quantify transport and deposition in small streams during high-flow events.
2. Evaluate the detectability of REE-labeled sediment experiencing resuspension in a subsequent high-flow event under amended channel conditions.

3. Estimate how far downstream REE-labeled sediments are transported in suspension and if time-integrated suspended sediment samplers can be used to track this movement.

Our study was conducted concurrently with a separate study that evaluated the effects of large wood (LW) on river-floodplain hydraulic connectivity within our study reach (Keys et al., 2018). LW was present in the study reach during the second of the two flood events; as such, these events represent unique conditions and do not represent replicate high-flow events. While we discuss the potential impacts of LW on sediment transport based on differing observations between Flood 1 and Flood 2, the study was not designed to test the impacts of LW on sediment transport.

Materials and Methods

Site Description

We conducted the study along Docs Branch, a first-order stream in Blacksburg, Virginia. The stream is in the Ridge and Valley physiographic province and is within the Virginia Tech Stream Research, Education, and Management Lab (StREAM Lab; Thompson et al., 2012; Keys et al., 2016). The focused portion of the study reach was approximately 60 m long and begins at a 0.91 m (3 ft) HL-type flume (Brakensiek et al., 1979) spanning the width of the reach (37° 12′ 20.40″ N, 80° 26′ 9.96″ W) and ends at an acoustic doppler velocimeter (SonTek Argonaut-SW, firmware version 9.3) installed in the streambed (fig. 1). The watershed upstream of the flume is approximately 100 ha and is primarily agricultural pasture. The stream has an average width of 0.93 m at bankfull and an average channel slope of 0.01 m m^{-1}.

Experimental Approach

We used REE-labeled sediments to explore sediment dynamics across two artificial flood events. Flood 1 relied on Lanthanum (La) labeled sediment as a tracer, while Flood 2 used sediment labeled with ytterbium (Yb) to track sediment movement. REE-labeled sediments were instantaneously

Figure 1. (a) Aerial view of study reach and (b) diagram of study reach showing sample locations.

injected into the head of the study reach at the initiation of each artificial flood. Surface water grab samples were collected at four cross-sections throughout the course of each flood to characterize fine sediment transport dynamics; depositional samples were collected in the channel and floodplain to better understand spatial heterogeneity in sediment deposition patterns; and time-integrated samples were collected in flow-through suspended sediment samplers to characterize the longitudinal transport of fine sediments. Sediment was collected from two locations immediately upstream of the experimental reach to determine background REE concentrations.

Labeling Sediment with REEs

To trace sediment movement, we collected and labeled sediments with REEs so that they could be distinguished from sediments already in the stream system; we injected the labeled sediments into the stream; and then we sampled water, the streambank, and the streambed to determine whether the detection of labeled sediments revealed clear transport and deposition patterns. Sediments for labeling were collected from a nearby streambank along the main stem of Stroubles Creek, 1 km from the study reach, and are mapped as the McGary (fine, mixed, active, mesic Aeric Epiaqualfs) and Purdy (fine, mixed, active, mesic Typic Endoaquults) series (NRCS, 2017). Sediments were sifted to remove particles greater than 2 mm and homogenized before mixing with 10 mmol of either lanthanum chloride ($LaCl_3 \cdot 7H_2O$; GFC Chemical) or ytterbium chloride ($YbCl_3 \cdot 6H_2O$; GFC Chemical) salt solutions at a 1:10 soil to solution ratio (4.8 kg soil + 48 L solution total; 1.6 kg of soil and 16 L of solution into each of three 18.9 L (5 gal) buckets). Kreider (2012) demonstrated that a 10 mmol L^{-1} solution provides maximum adsorption of the tracer without leaving excess REEs in solution. The sediment/salt solution was stirred by hand for approximately 3 min three times on alternate days for 5 d and then allowed to settle for 8 d before decanting the supernatant water.

Generation of Flood Events

We generated the two artificial flood events by blocking road culverts located 25 m upstream of the flume to create a small backwater pond, followed by rapid removal of the blockage. A test flood was generated prior to the experiment (23 May 2016) to determine the extent of backwatering required to achieve the desired flooding (defined by the minimum flow rate) and to wet the floodplain soils so that similar antecedent soil moisture conditions would be present for the subsequent experimental floods.

For Flood 1 (24 May 2016), we quickly injected La-labeled sediments (4.7 kg in stream water slurry) into the outfall nappe of the HL flume as the flood pulse reached the flume. By design, all surface water flow was directed through the flume. Flood 2 (25 May 2016) was generated after placing LW at three locations within the channel (fig. 1b). The LW at each location consisted of a single root wad and attached trunk (see Keys et al., 2018 for additional details). For Flood 2, we injected Yb-labeled sediments (4.7 kg in stream water slurry) into the HL flume nappe.

Sediment Sampling

Transport in Suspension

Four sampling cross-sections were established throughout the reach (XS1 through XS4, fig. 1b). The cross-sections were surveyed to generate elevation profiles. We measured suspended sediment transport by continuously collecting water samples throughout the flood flows using small gas-powered pumps (Echo WP-1000) at cross-sections XS1, XS3, and XS4. A pump was installed at XS2, but pump failure precluded the collection of samples from this cross-section. The sample intakes were fixed to a point in the channel that was submerged under baseflow conditions, within the deepest part of the cross-section, and elevated from the streambed enough to prevent sampling of bed sediments when the pump was activated (approx. 5 cm above the streambed). This sampling approach was designed to satisfy as many guidelines of the field methods for measurement of fluvial sediment (Edwards and Glysson, 1999) as possible while minimizing the effects of guidelines that could not be satisfied. Samples of total suspended solids (TSS) were collected by drawing stream water into prelabeled 18.9 L (5 gal) buckets. Sample collection began when water levels at the given sample station began to visibly rise. Time of sample initiation was noted (precision to 1 min), and buckets were filled sequentially at 30 s intervals for the first 2 min and at 1 min intervals thereafter, until 12 buckets had been filled (~10 min total sampling period). We then placed lids on the buckets for transport to the laboratory for processing.

Following collection, each combined bucket, lid, and water sample was weighed to the nearest 28 g (1 oz) on a Detecto scale (model 2201AD) and then allowed to sit quiescent for a minimum of 5 d, which is an order of magnitude longer than the time required for clay particles (<4 μm in diameter) to settle in still water with the depth of the sampling buckets. Following this settling period, clear water was decanted from each bucket until a depth of approximately 10 cm remained above the settled sediment. Additional water was siphoned off using a Geopump peristaltic pump (GeoTech EasyLoad II, high performance, model 900-1280) until approximately 2 cm of water remained above the sediment layer. The bucket was then agitated to form a sediment/water slurry that was decanted to labeled 1 L containers. The buckets were rinsed with a minimal volume of tap water to wash any remaining sediments into the 1 L containers. The 1 L sample containers sat undisturbed for a minimum of 2 d, at which point the overlying water was siphoned off to a depth of less than 1 cm. The containers were then placed in a drying oven at 60°C for 2 d or until dry, and sediments were weighed to the nearest 0.01 g. Finally, sediments were homogenized by hand, or using a mortar and pestle, and then analyzed for REEs and particle size as detailed below.

The labeled buckets and their accompanying lids were rinsed, allowed to air dry, and weighed to the nearest 28 g (1 oz) so that the approximate volume (L) of water in each sample could be calculated as follows:

$$VOL = (M_{WBL} - M_{BL}) \times (1/1000) \quad (1)$$

where

VOL = final water volume (L)

M_{WBL} = mass of water, bucket, and lid (g)

M_{BL} = mass of bucket and lid (g).

TSS concentrations were calculated by dividing the total dry sediment mass per sample by the sample volume (g L^{-1}). Sediment breakthrough curves were generated by graphing TSS over time for each cross-section.

Deposition

Sediment deposition was measured using a modified version of the turf mat approach described by Von Bertrab et al. (2013). We anchored artificial turf mats (15 cm^2) with landscape pins in triplicate in the thalweg and nearshore floodplain (on the vegetated streambank within 0.3 m from the water's edge) at XS1, XS2, and XS3 prior to backwatering for each flood event. The mats were intermediate in texture between the relatively smooth streambed and the vegetated floodplain. This artificial turf mat approach is commonly used to evaluate sediment deposition in floodplains (e.g., Baborowski et al., 2007; Maaß and Schüttrumpf, 2019). The morning following each flood, following a return to baseflow conditions (~0.7 L s^{-1}), the mats were collected and gently transferred into zip closure bags. The mats were rinsed to collect sediments in labeled 1 L containers, and the dry mass of collected sediment was measured to an accuracy of 0.01 g after drying for two days at 60°C. Sample REE concentrations and particle sizes were analyzed as detailed below after combining the triplicate mats into a single sample to provide sufficient mass for analysis.

Longitudinal Transport

Flow-through suspended sediment samplers were established 90 m downstream of the flume for Flood 1 and at both 90 m and 850 m downstream of the flume for Flood 2. The samplers were based on a design by Phillips et al. (2000) and were deployed in triplicate at each location with inlets set approximately 2 cm above baseflow. These samplers collected suspended sediments from waters that flowed through the samplers when the flood stage was at or above the level of the inflow point and provide time-integrated measurements of suspended sediment transport. These samplers were used to determine if labeled sediments had been transported downstream in suspension as far as the sampler locations during the floods. After the flow events, trapped sediments were collected by rinsing the flow-through samplers and collecting the resulting sediment slurry in 1 L containers. The sample containers were allowed to sit undisturbed for a minimum of 2 d, at which point the overlying water was siphoned off to a depth of less than 1 cm. The containers were placed in a drying oven at 60°C for 2 d or until dry, and sediments were weighed to the nearest 0.01 g. Samples from the triplicate suspended sediment samplers were combined to allow sufficient mass for analysis of REE concentrations and particle sizes.

Analysis of REE Concentrations and Particle Sizes

Sediment REE concentrations were analyzed in samples collected from background locations, sediment tracers, and at each sample location. Background concentrations established a baseline to distinguish between injected sediment concentrations and those naturally occurring in the study reach. Dried samples were homogenized by hand or with a mortar and pestle to separate particles. A 0.5 g portion of each sample was digested with 10 mL of concentrated nitric acid following USEPA Method 3051A (USEPA, 2007) using a MARS Xpress laboratory-grade microwave. REE concentrations in the digestate were analyzed at the Civil and Environmental Engineering Lab at Virginia Tech via inductively coupled plasma - mass spectrophotometry (ICP-MS) following USEPA Method 6020A (USEPA, 1998). The minimum reporting level was 0.1 ppb (corresponding to sediment concentrations of 0.33 mg kg^{-1} for the sediment sample mass and dilution used here).

Particle sizes were evaluated for each sample using a CILAS 1190 particle size analyzer and associated Size Expert software (CILAS, 2014). Samples were analyzed after mixing 1.0 g of sample with 20 mL of distilled water and agitating overnight.

Estimation of Flow

Hydrographs at XS1 during Flood 1 and Flood 2 were generated using flows calculated from the HL flume based on flow depth within the flume (measured with a pressure transducer) and standard flow equations for 0.9 m (3 ft) HL flumes (Brakensiek et al., 1979). Data from the acoustic doppler velocimeter, located as XS3, were used to generate hydrographs for this cross-section. See Keys et al. (2018) for additional details on the reach hydrodynamics.

Estimation of Total Sediment and Tracer Transport in Suspension

We estimated the total mass of sediment passing a cross-section within the 10 min sampling period separately for XS1 and XS3 using the following equation:

$$SED_{totSUS} = \sum_{i=1}^{12} \mathrm{TSS} \times Q \times T \tag{2}$$

where

SED_{totSUS} = total mass of sediment passing the cross-section (g)

i = sampling interval

TSS = total suspended solids (g L^{-1})

Q = flow rate (L s^{-1})

T = time between samples (s).

Because TSS was not quantified at XS2 and flow was not quantified at XS4 (down-gradient of the acoustic doppler velocimeter), total sediment transported could not be calculated for those cross-sections. The total mass of REE tracer passing XS1 and XS3 within the 10 min sample collection period was estimated as follows:

$$SED_{tracer\_sum} = \sum_{i=1}^{12} SED_{totSUS} \times \frac{\left(REE_{CONCtot} - REE_{CONClocal}\right)}{\left(REE_{CONCtracer} - REE_{CONClocal}\right)} \tag{3}$$

where

SED_{tracer_sum} = total REE-labeled sediment passing the cross-section (kg)

i = sampling interval

SED_{totSUS} = total sediment passing the cross-section during the sampling interval (kg)
$REE_{CONCtot}$ = concentration of La or Yb in the TSS sample (mg kg^{-1})
$REE_{CONClocal}$ = background concentration of REEs
$REE_{CONCtracer}$ = concentration of REEs in the sediment tracer.

Estimation of Sediment and Tracer Deposition

We estimated total sediment deposition in the channel for three segments (flume to XS1, XS1 to XS2, and XS2 to XS3) by multiplying the surface area of the segment by the average mass deposited. The area of each segment was calculated as the length along the thalweg times the bankfull width of 0.93 m. Deposition for the stream segment from the flume to XS1 was estimated as the average deposition on channel sample mats from XS1. Deposition from segment XS1 to XS2 was estimated as the average deposition on channel sample mats from XS1 and XS2. Similarly, deposition from segment XS2 to XS3 was estimated as the average deposition on sample mats from XS2 and XS3.

Floodplain deposition was calculated similar to channel deposition for the three segments. Because the deposition mats in the floodplain were located within 0.3 m from the streambank, and deposition was expected to be greater closer to the channel, we estimated floodplain deposition for a 0.5 m band along the right side of the channel rather than for the entire area of inundation. Because of topography, the floodplain stream right (i.e., right side looking downstream) was inundated before the left bank was breached (fig. 2), necessitating a focus solely on the right side of the channel. This approach likely underestimated total floodplain deposition; however, the alternative approach (i.e., assuming that our deposition data were representative of the entire area of inundation) would have greatly overestimated actual deposition in the floodplain.

The total mass of REE tracer deposited on the sample mats was estimated as follows:

$$SED_{tracer} = SED_{totMAT} \times \frac{\left(REE_{CONCtot} - REE_{CONClocal}\right)}{\left(REE_{CONCtracer} - REE_{CONClocal}\right)} \quad (4)$$

where
SED_{tracer} = mass of tracer deposited on mats (g)
SED_{totMAT} = total sediment deposited on mat (average of 3 mats, g)
$REE_{CONCtot}$ = concentration of La or Yb (three mats homogenized into one sample, mg kg^{-1})
$REE_{CONClocal}$ = background concentration of REE
$REE_{CONCtracer}$ = concentration of REEs in sediment tracer.

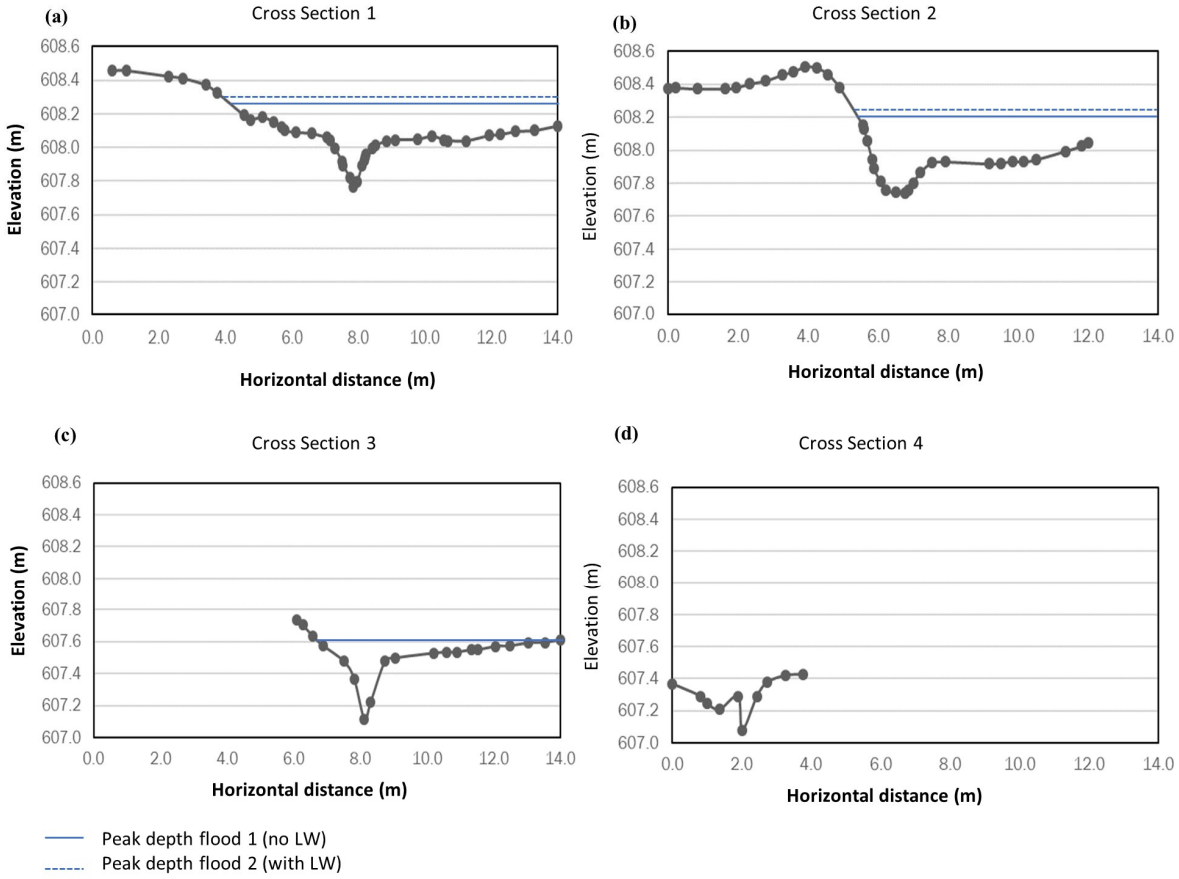

Figure 2. Cross-section elevations viewed from upstream to downstream. Solid blue lines indicate peak depths during Flood 1 (0.47, 0.47, and 0.48 m for cross-sections 1, 2, and 3, respectively). Dotted blue lines indicate peak depths during Flood 2 (0.5, 0.5, and 0.48 m, respectively). Peak depth at cross-section 3 was equivalent for Flood 1 and Flood 2. Flow data were not available for cross-section 4.

Data Analysis and Statistics

Transport in Suspension

We compared the magnitude and timing of sediment breakthrough curves to evaluate the effects of LW and distance from loading point (i.e., distance from the flume; variable = XS) on the transport of sediment in suspension. We calculated average transport velocities by dividing the distance traveled (distance of cross-section from the HL flume sediment injection point) by the time to the peak of the sediment pulse (maximum measured TSS concentration) at each cross-section. TSS data and flow data for XS1 and XS3 were used to evaluate hysteresis at these cross-sections.

Deposition

The effects of LW (i.e., Flood 1 with no LW, Flood 2 with LW), XS (i.e., distance traveled), and location (LOC, i.e., channel or floodplain), and each two-way interaction on sediment deposition (g cm^{-2}) were evaluated using ANOVA. Deposition data were log_{10} transformed to meet normality assumptions prior to analysis and confirmed via the Shapiro-Wilks test. Pairwise differences were evaluated with Tukey's honestly significant differences tests. For this and all subsequent tests, Type I error was set at $\alpha = 0.05$.

Results and Discussion

REE Concentrations and Particle Size of Labeled Sediments

Labeled sediments contained REEs at levels of 7,193 mg kg^{-1} (La) and 8,152 mg kg^{-1} (Yb), which was estimated as 3 to 4 orders of magnitude greater than background levels (21.5 mg kg^{-1} for La, 1.0 mg kg^{-1} for Yb). Labeled sediments were representative of the silt class (median diameter D_{50} = 16.7 µm, D_{10} = 1.9 µm, and D_{90} = 70.9 µm).

Artificial Flood Events

Because the artificial floods were generated by blocking streamflow at the upstream culverts, minimum flows before the removal of the blockage were 0 L s^{-1} at the HL flume for both Flood 1 and Flood 2. Both floods reached approximately 55 L s^{-1} peak flow and had similar hydrographs at the upstream end of the study reach (fig. 3). Using regional curves for streams in the non-urban Ridge and Valley province (Keaton et al., 2005), the estimated 1.5 year return period flow event for a 100 ha watershed is 515 L s^{-1}. This is approximately 9 times the flows generated in our experimental floods. Therefore, based on historical rainfall/runoff data collected at the site, flows similar to our experimental event occur multiple times per year and inundate the existing inset floodplains. Data from the pressure transducer at the HL flume indicated that 7.4% of daily average flows for the 2016 calendar year exceeded 55 L s^{-1}. While the hydrographs for XS1 were similar for Flood 1 and Flood 2, the hydrographs for XS3 reflected reduced flow rates and a delay of the flood pulse reaching this cross-section when LW was present in the channel.

Transport in Suspension

Suspended sediment transport was dampened and delayed when LW was present in the channel (Flood 2) relative to when the channel was clear (Flood 1; fig. 4). This observation may in part reflect a lower availability of transportable sediment during Flood 2 following scour occurring during Flood 1. The total TSS pulse (quantified by the maximum TSS concentrations in the channel) passed XS1 (upstream of LW) during the first 1.5 min of both floods. In the absence of LW (Flood 1), the TSS pulse reached the farthest downstream sampling point (XS4) at 5.5 min, equating to a transport velocity of 0.25 m s^{-1}. With LW (Flood 2), the TSS pulse reached XS4 at 7.5 min, corresponding to a transport velocity of 0.18 m s^{-1}. This decrease in transport velocities due to LW agrees with the model results reported by Keys et al. (2018). The transport of REE-labeled sediment was identical to that of TSS, which may be because the D_{50} of the total sediment transported (13.85 to 53.65 µm) was similar to the D_{50} of the labeled sediment (16.7 µm). In streams that have a larger variance in water column particle size classes, we would expect differences in transport velocities for particles of substantially different size classes. The transport velocities measured here for silt are less than the 1 m s^{-1} sediment transport velocity per "event" assumed by Pizzuto et al. (2014); however, their estimate was based on >1.5 year events, while our experimental flows were <1 year events. Moreover, Pizzuto et al. (2014) focused on watersheds that are as much as 100 times larger than our study watershed; as such, our smaller transport velocities are not unexpected.

The total mass of sediment passing XS1 and XS3 in suspension exceeded the mass injected into the channel during both floods (table 1), indicating entrainment of sediments bedded within or above the study reach. Less total sediment

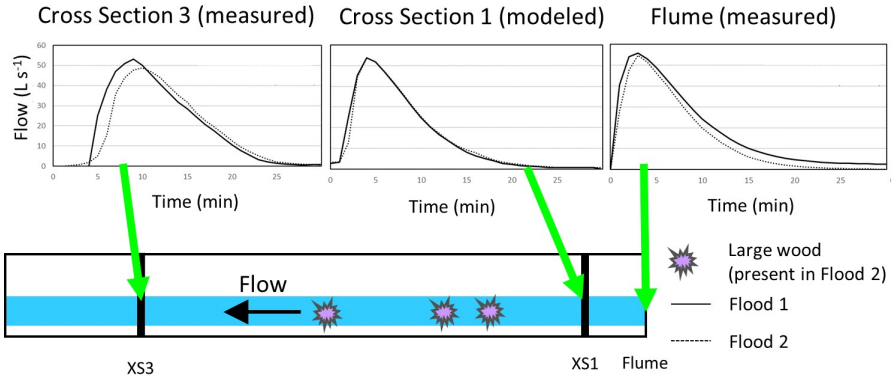

Figure 3. Comparative hydrographs for Flood 1 and Flood 2 at the HL flume, cross-section 1 (XS1), and the acoustic doppler velocimeter (ADV) located at cross-section 3 (XS3).

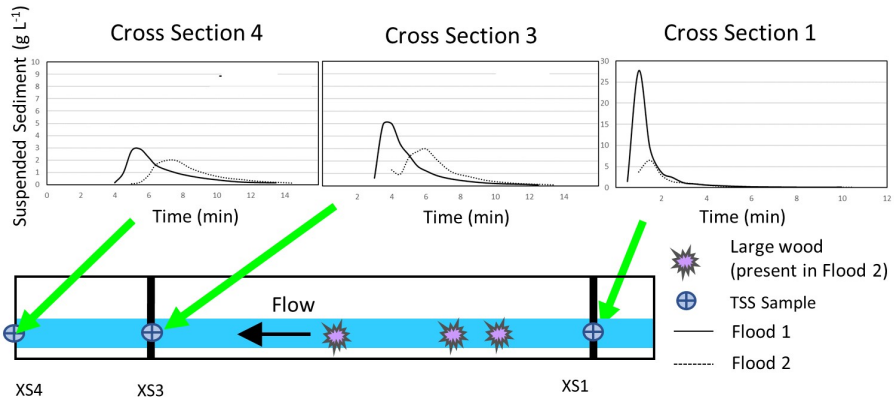

Figure 4. Comparative total suspended solids (TSS) concentrations for Flood 1 and Flood 2 at cross-section 1 (XS1), cross-section 3 (XS3), and cross-section 4 (XS4). Note the expanded scale for XS1.

Table 1. Percentages of injected sediment tracer passing cross-sections in suspension.

Flood	Cross-Section	SED_{total} (kg)[a]	SED_{tracer} (kg)[b]	Percentage Passing[c]
1	XS1	17.16	0.65	14%
	XS3	21.14	0.82	17%
2	XS1	9.03	0.43	9%
	XS3	12.50	0.69	15%

[a] SED_{total} = total sediment passing cross-section.
[b] SED_{tracer} = total tracer sediment passing cross-section (La-labeled in Flood 1, and Yb-labeled in Flood 2).
[c] Percentage of the mass of tracer injected into the stream that traveled past the cross-section in suspension.

was transported in suspension in Flood 2 than in Flood 1 for both XS1 (upstream of LW placement) and XS3 (downstream of the LW), suggesting that scouring and sediment transport during Flood 1 may have reduced the sediment subsequently available for transport. Therefore, the total sediment transported reflects the impacts of both sediment availability and the effects of LW on transport.

Consistent with expectations, positive (clockwise) hysteresis was observed at XS1 and XS3 during both Flood 1 and Flood 2, indicating that the sediment pulse preceded the flood peak (fig. 5). Positive hysteresis is commonly observed when the sediment supply is depleted over the course of a flow event (Naden, 2010).

REE-labeled sediment was recovered in all TSS samples, demonstrating the potential use of this labeling approach to measure the transport of specific sediments of interest (e.g., size class). Approximately 0.65 kg (14%) of the 4.7 kg of La-labeled sediment injected in Flood 1 passed XS1 in solution (table 1). This suggests that the remaining 86% of the injected sediment entered storage (either in the channel bed or floodplain) within 9.5 m of the study reach. This estimate was similar to the findings of Mahler et al. (1998), who traced suspended transport of neodymium-labeled clay in a "small urban creek" and estimated that only 21% of the total injected sediment traveled 15 m at 6.3 L s^{-1} uniform flow. While our flow rates were much higher than those of Mahler et al. (1998), they were nearly an order of magnitude less than bankfull flows. As such, our low proportion of estimated transport in solution may be consistent with the expectations of Pizzuto et al. (2014), who theorized that events that produce less than bankfull flows do not contribute significantly to downstream sediment transport. That said, the volumes and distances of sediment transported that are "significant" in terms of biological and physical stream health have not yet been determined.

Interestingly, a higher percentage (17%) of the injected La tracer appeared to pass XS3 than passed XS1 in solution in Flood 1 (table 1). This may be an artifact of the location of the TSS sampling point (in the thalweg, 5 cm above the streambed). This sampling strategy may have been more likely to capture entrained unlabeled bottom sediments instead of the silt-sized labeled sediment traveling at a higher depth in the water column. A depth-integrated sampling approach is likely to provide a more representative sample of sediment in suspension (Edwards and Glysson, 1999); however, this approach was not feasible due to the small size of our study reach and the rapid nature and changing conditions of the sampling event. In addition, we did not sample suspended sediments in the lateral floodplain, which may have had higher concentrations of the injected fine sediment particles than the main channel. Cross-section data overlaid with peak flow depths (fig. 2) show that, based on topography, a higher proportion of the water at XS1 flows across the floodplain, resulting in higher flow heterogeneity (and associated higher heterogeneity in sediment transport across the cross-section). In contrast, XS3 flows were more concentrated in the channel; therefore, TSS measurements for XS3 should be more representative of the true cross-section average values than those at XS1. These finding and our estimates of deposition (below) highlight the spatial complexity of sediment transport and deposition even within single high-flow events.

Observed patterns were similar for Flood 2; the estimate of Yb-labeled tracer passing XS1 (9%; table 1) was less than the estimate of tracer passing XS3 (15%). The greater differential between these two estimates in Flood 2 reflects deeper flows (fig. 2) and therefore greater differences between cross-section average TSS and the TSS measured at the thalweg sampling point.

The La concentrations in the suspended sediment collected during Flood 2 exceeded background concentrations (fig. 3c). This demonstrates that a portion of the sediment that had been deposited during Flood 1 was entrained and transported in suspension during the subsequent flood and

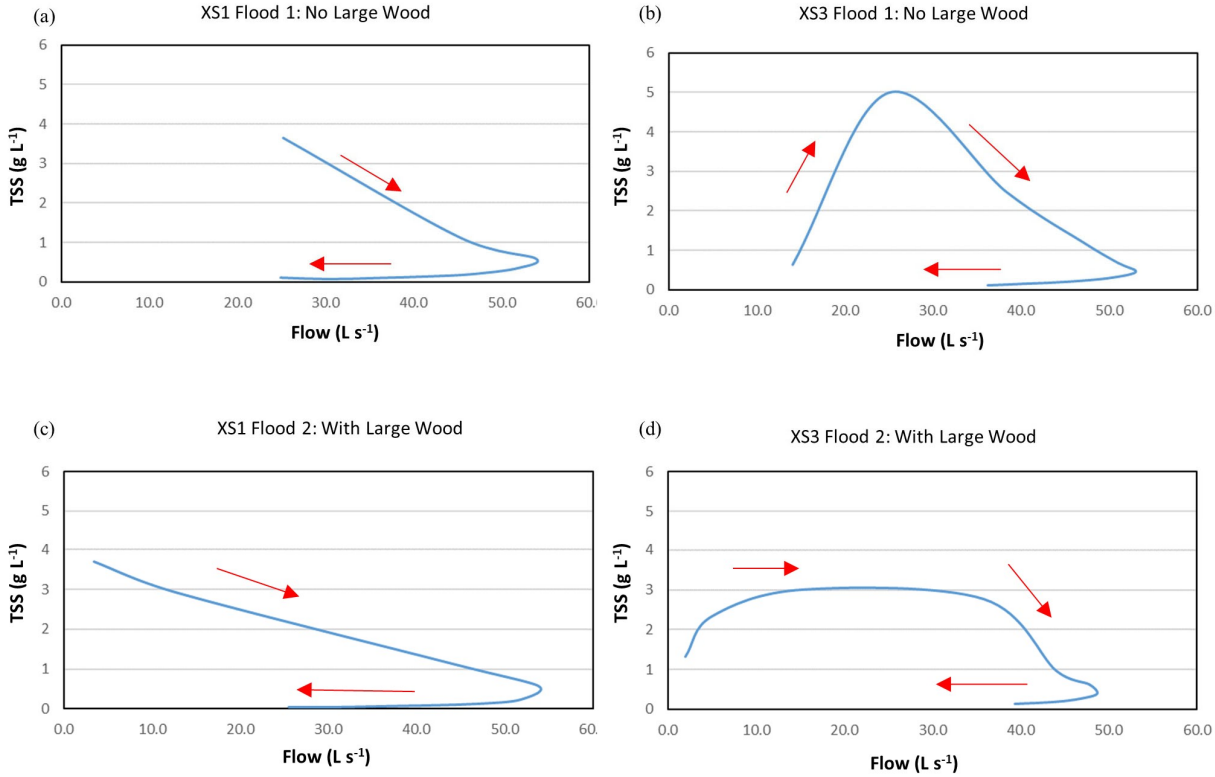

Figure 5. Positive hysteresis for total suspended solids (TSS) transport at cross-sections 1 (XS1) and 3 (XS3). Arrows indicate direction of time.

indicates the value of using multiple REEs in a series of events to detect resuspension. Few studies have measured in-channel fine sediment remobilization during artificial flood events. Muirhead et al. (2004) evaluated resuspension of in-channel fecal bacteria (associated with deposited sediments) during an artificial flood in an agricultural stream, and Harvey et al. (2012) used latex particles to demonstrate entrainment of in-channel fine particles during an artificial flood in a Coastal Plain stream.

While TSS levels decreased overall with distance downstream (fig. 4), the concentration of REEs in suspension increased (fig. 6). This may reflect the increase in the proportion of finer sediment carried in transport at down-gradient locations as larger particles settled out of the system, as recorded in the shifting particle size distributions.

Sediment Deposition

Sediment deposition per unit area in the stream channel was greater overall than deposition in the floodplain during both floods (LOC $p < 0.001$, df = 1, $n = 36$). This effect was driven by depositional differences at XS1 and XS2 closest to the flume; deposition was equal in the channel and floodplain at XS3 (fig. 7). Even though roughness was higher in the floodplain, we found greater deposition per unit area in the channel because much more of the sediment-laden flows were within the channel, with only a small fraction entering the floodplain area. This depositional pattern may be attributable to the study design, which mimicked a dam break with sediment inputs limited to alluvial sources rather than lateral inputs from overland flow or tributaries, which would occur during a natural runoff event (Foley et al., 2017).

Of the 4.7 kg of La tracer injected into the stream during Flood 1, we estimate that 5.8% was deposited in the channel within the first 0.95 m (distance to XS1), and another 6.4% was deposited in the near floodplain (0.5 m band on the right bank) (table 2). Summing deposition from the flume to XS3, we estimate that 20.4% of the La tracer was deposited in the channel, and another 20.4% was deposited in the near floodplain. As discussed previously, 17% of the La tracer was estimated to pass XS3 in solution. Together these account for approximately 58% of the injected tracer by XS3.

Channel deposition was greater for Flood 2 than Flood 1, with deposition of Yb tracer from the flume to XS3 representing 26.1% of the injected sediment. Greater deposition within the channel may reflect reduced flow rates in the main channel in the presence of LW, which is consistent with the findings of Drummond et al. (2020), who demonstrated greater fine particle retention in a restored reach containing LW than in a control reach. Near-floodplain deposition in Flood 2 was slightly lower than in Flood 1 at 18.0%. Reduced near-floodplain deposition may result from higher lateral flows with LW in the channel, which would be expected to transport fine sediment transport farther into the floodplain.

Given the 15% amount of Yb tracer estimated to pass XS3 in solution (discussed previously), 59% of the tracer injected during Flood 2 was accounted for by XS3. It is worth nothing that the La-labeled sediments deposited in both channel and floodplain samples were recovered after Flood 2 (table 2), which implies that some portion of the sediments deposited during Flood 1 was resuspended and resettled during Flood 2.

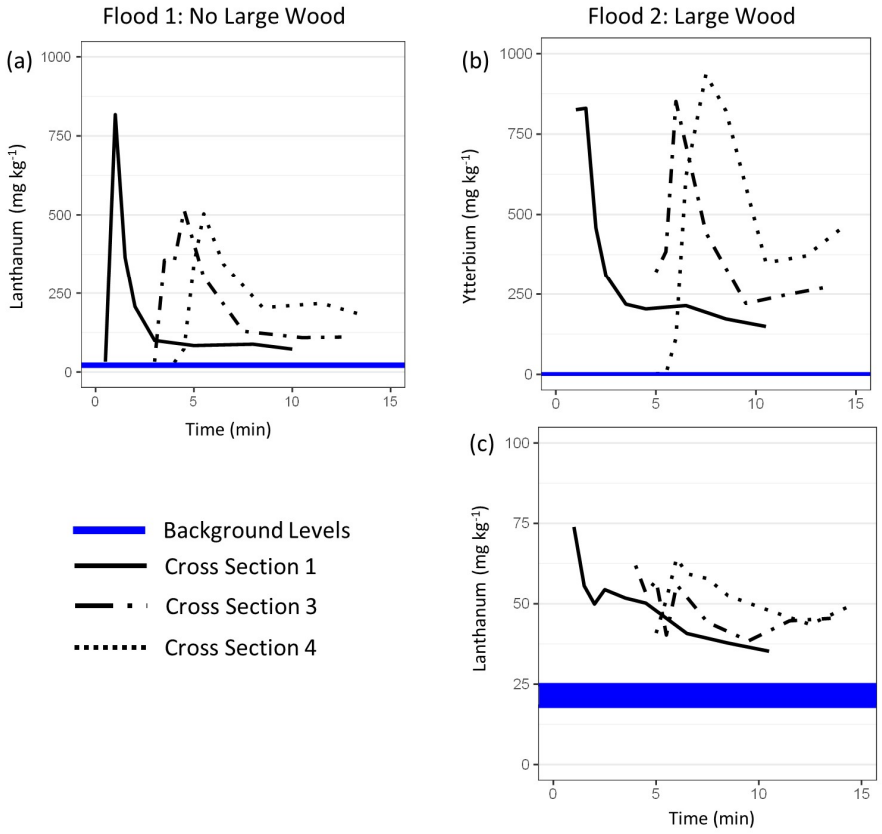

Figure 6. Lanthanum and ytterbium concentrations in suspended sediment samples collected over the course of the flood events at cross-sections 1, 3, and 4. Note the reduced scale for lanthanum during Flood 2.

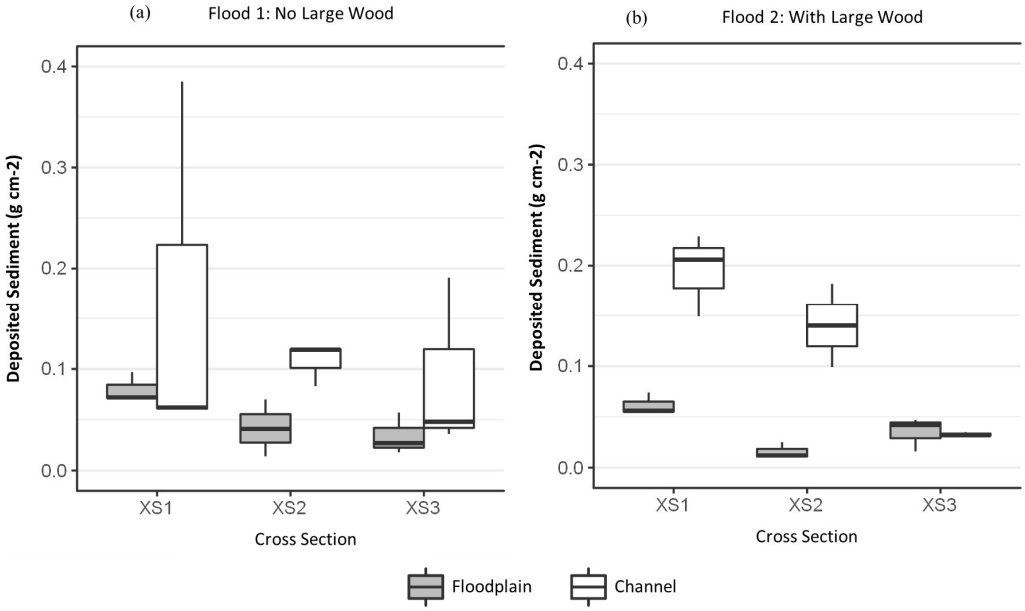

Figure 7. Deposited sediment per unit area in Flood 1 and Flood 2.

Approximately 40% of the injected sediment was unaccounted for at XS3 for both floods. Errors in suspended transport estimates could have resulted from the reliance on collection of sediment from the single sampling location in the water column. Sediment deposition in the floodplain was underestimated because only near-floodplain deposition was quantified. Regardless, based on the data presented, sediment deposition exceeds transport during "moderate" flow events (defined here as flow intermediate to baseflow and bankfull flow), such as those represented in our experimental floods, which has substantial implications for lag time estimates.

Table 2. Percentage of injected sediment tracers deposited in study reach.

Flood 1 Deposition			Percentage of La tracer injected in Flood 1 that was deposited in each segment			
Segment	Length		Channel	Floodplain		
Flume to XS1	0.95 m		5.8%	6.4%		
XS1 to XS2	2.35 m		9.9%	9.6%		
XS2 to XS3	3.58 m		4.6%	4.4%		
		Sum:	20.4%	20.4%		
Flood 2 Deposition			Percentage of La tracer injected in Flood 1 that was deposited in each segment		Percentage of Yb tracer injected in Flood 2 that was deposited in each segment	
Segment	Length		Channel	Floodplain	Channel	Floodplain
Flume to XS1	0.95 m		2.4%	0.5%	10.2%	6.3%
XS1 to XS2	2.35 m		3.2%	0.7%	13.6%	8.8%
XS2 to XS3	3.58 m		0.6%	0.5%	2.3%	2.9%
		Sum:	6.1%	1.7%	26.1%	18.0%

LONGITUDINAL TRANSPORT

REE-labeled sediments were detected in the down-gradient time-integrated suspended sediment samplers after both floods (samplers located at 90 m downstream for Flood 1 and at 90 m and 850 m downstream for Flood 2). In Flood 1, 11.68 g of sediment with a tracer (La) concentration of 258 mg kg^{-1} was collected in the sampler 90 m downstream; this concentration was greater than background levels but less than the concentrations of the labeled sediment, indicating that it represents a mix of injected and entrained sediments. During Flood 2, 11.91 g of sediment with a Yb concentration 443.3 mg kg^{-1} was collected. This concentration was similarly intermediate to background levels and the concentrations in the labeled sediment. In Flood 2, the La concentrations in the sediment collected from the time-integrated samplers also exceeded background concentrations, indicating that both particles newly introduced in suspension (Yb tracer) and previously deposited particles that were newly entrained (La tracer) were flushed from the study reach. The combination of REEs and longitudinal TSS samplers provided information on the distance a particle is transported before entering storage (i.e., L_s, or characteristic length scale, in the sense of Pizzuto et al., 2014). In our study, we demonstrated the transport of silt at least 850 m in a moderate flow event.

EFFECTIVENESS OF REES AS TRACERS

Ideal sediment tracers should have strong soil binding properties, high analytical sensitivity, easy and inexpensive analytical requirements, low environmental background concentrations, no interference with sediment transport, no negative environmental effects, and various forms with similar but distinguishable properties that can be used for tracking (Zhang et al., 2001; Guzmán et al., 2013). The labeling of local streambank sediments with REEs for this study was straightforward and required no special equipment. Kreider (2012) demonstrated strong retention of La and Yb to sediment from the same location as ours (99.97% and 99.71% for La and Yb, respectively, following five washes with stream water). REEs in this study were detected at a minimum reporting level of 0.33 mg kg^{-1} following standard acid digestion and ICP-MS techniques. Although REEs have specific gravities (La = 6.15; Yb = 6.96) that are 2 to 3 times that of most inorganic soils (which range from 2.6 to 2.8; Department of the Army, 1999), we assumed that there was no significant interference with sediment transport. Aquatic toxicity studies on these elements suggest that physical and oxidative damage to algal cells is possible from unbound REE oxides (Guida et al., 2017). However, due to their strong sediment-binding capacity, REEs used as sediment tracers are unlikely to become biologically available. Finally, the lanthanide series contains 15 elements with similar chemical traits that are analytically differentiable, which provides multiple possibilities to use these elements experimentally. These include targeting specific portions of the sediment distribution (i.e., sands, silts, or clays) or tracking sediment through multiple floods that vary in magnitude. As our results highlight, spatially intensive sampling may be required to develop a more detailed characterization of sediment fate and transport.

CONTRIBUTIONS TO CHARACTERIZATION OF FLUVIAL SEDIMENT DYNAMICS

The results of our tracer study show that REE-labeled sediments can be used to obtain transport parameter estimates useful for sediment and contaminant transport studies and models, such as sediment transport velocity, TSS for specific sediment size classes, and maximum distance traveled. In addition, the use of REEs for labeling sediments in consecutive floods allowed clear identification of sediment transport and deposition in both the stream channel and floodplain. The REE-based tracer technique enabled estimation of transport distances for silt particles during moderate flow events ranging from 0 m (La-labeled sediment deposited, resuspended, and deposited again in XS1 over two flow events) to greater than 850 m (Yb-labeled sediment detected in the farthest down-gradient sampler after a single flow event). This also confirms that both storage and particle exchange were occurring.

We estimated that approximately 41% of the sediment tracer deposited either in the channel or near-floodplain within the first 69 m of our study reach. While we were able to detect the La tracer in both flood events, the concentrations in Flood 2 had returned to levels only slightly elevated to background. This suggests that a single REE tracer may only be detectable over a limited time period, particularly when studied at elevated flows. It is critical to account for the heterogenous distribution of sediment with depth in the water column and between channel and floodplain when designing sampling schemes. The ability to visualize resuspension in this system is novel and contrasts with findings from an ephemeral semi-arid basin in which an erosional study

suggested little redeposition and, therefore, effective transport in suspension through the system (Polyakov et al., 2009).

Data derived from future REE tracer studies could be used to characterize reach-scale to watershed-scale sediment dynamics, including the travel time of the sediment pulse, the leading edge and peak transport or centroid, and information on relative suspension and deposition levels. Unique insights may be gained via the tracking of labeled sediments in a second storm event (i.e., the event following tracer injection). Relative rates of storage and transport in subsequent flow events would provide data to both develop and validate models of transport decay rates.

In this study, we injected sediments with REE concentrations that were 3 to 4 orders of magnitude greater than background levels. The maximum concentrations collected in both deposited and suspended sediment samples were at least an order of magnitude less than the injected concentrations in the first flood following injection and dropped by an additional order of magnitude for suspended samples during the second flood (i.e., for La-labeled sediments shown here). Depositional concentrations of La-labeled sediment in Flood 2 were approximately 3 times less than the levels seen in Flood 1. These data suggest that a single labeled cohort of sediment particles can only be tracked through a limited number of sequential storm events, likely dependent on the ability of the sediment to adsorb the tracer, the mass of labeled sediment added to the system, and the size of the study reach.

Understanding Lag Time in Watershed Management

The temporal lag between an action (BMP implementation) and response (improved water quality downstream) is one of the biggest uncertainties in watershed management programs (Meals et al., 2010; CBPSTAC, 2013; Pizzuto, 2014). In this study, we focused on lag times in relation to sediment, but similar issues exist for other pollutants, such as nutrients and contaminants (Zhang et al., 2016; Van Meter et al., 2018). Efforts to address lag times have been discussed as part of the Chesapeake Bay Program (through incorporation into the Chesapeake Bay Watershed Model) and estimated as part of theoretical frameworks that incorporate estimates of suspended sediment length scales and travel velocities (e.g., Pizzuto et al., 2014). However, these frameworks do not characterize the distribution of sediment at both the reach and watershed scale.

The results from our study support a growing body of literature that characterizes the fate and transport of fine sediments through watersheds. We were able to quantify actual sediment pulse velocities and measure discrete transport distances during experimental floods in a small stream. The REEs allowed us to characterize sediment movement within the relatively short study reach, such that even if individual particles remained in the reach, entrainment, transport, and deposition within the smaller reach were still evident. This may have important implications for the impacts of sub-bankfull storm events on fine sediment and the resulting ecosystem functions important for watershed management, such as stream metabolism (Larsen and Harvey, 2017), pathogen transport (Drummond et al., 2015), and regional carbon cycling (Cole et al., 2007). Further studies are needed to truly estimate sediment lag times for use in watershed management and assessment activities.

Conclusions and Recommendations

The results of this study demonstrated the use of REE-labeled sediments to track fluvial particle movement, which may prove to be a particularly useful strategy for studies at the reach scale. Future work should include additional depositional studies to expand understanding of floodplain deposition using higher flows, as well as more spatial sampling to quantify the heterogeneous nature of floodplains (in terms of roughness and topographical variability). This method could be used to begin to close the current knowledge gap between moderate flows and single-event, short-term sediment transport compared to long-term, averaged measures such as those of Pizzuto et al. (2014). Our work illustrates the large variation in sediment particle fate and transport within even a single flow event and relatively small reach, so future work should incorporate a larger number of sampling points when possible. Additional data of this nature in combination with research on longer reach lengths and time scales are needed to fully close the gap between single-event and long-term sediment transport, which is necessary for a fuller understanding of lag times.

Acknowledgements

The authors declare no conflicts of interest. This work was completed with funding from the Virginia Tech Graduate School, the Virginia Tech Global Change Center, the Virginia Water Resources Research Center, as well as the Virginia Agricultural Experiment Station and the Hatch Program of the USDA National Institute of Food and Agriculture. Valuable field and laboratory assistance was provided by members of the Hession and Krometis research teams and by Michael Wojdak. Special thanks to Laura Lehmann and Dumitru Branisteanu, who were instrumental in setting up the experimental flood events. The manuscript was improved by comments from Paul Angermeier and Larry Willis. Finally, this research would not have been possible without the intellectual advances and methods developed as part of a grant from the Canaan Valley Institute (CVI 2010-06) with additional support from the USDA Agricultural Research Service office at Penn State (collaborators: Tyler Kreider, Kevin McGuire, Brian Strahm, Cully Hession, Tony Buda, and Danny Welsch).

References

Åberg, E. U., & Tapsell, S. (2013). Revisiting the River Skerne: The long-term social benefits of river rehabilitation. *Landscape Urban Plan., 113*, 94-103. https://doi.org/10.1016/j.landurbplan.2013.01.009

Baborowski, M., Büttner, O., Morgenstern, P., Krüger, F., Lobe, I., Rupp, H., & Tümpling, W. v. (2007). Spatial and temporal variability of sediment deposition on artificial-lawn traps in a

floodplain of the River Elbe. *Environ. Pollut., 148*(3), 770-778. https://doi.org/10.1016/j.envpol.2007.01.032

Bertoni, D., Sarti, G., Benelli, G., Pozzebon, A., & Raguseo, G. (2010). Radio frequency identification (RFID) technology applied to the definition of underwater and subaerial coarse sediment movement. *Sediment. Geol., 228*(3), 140-150. https://doi.org/10.1016/j.sedgeo.2010.04.007

Black, E., Renshaw, C. E., Magilligan, F. J., Kaste, J. M., Dade, W. B., & Landis, J. D. (2010). Determining lateral migration rates of meandering rivers using fallout radionuclides. *Geomorphol., 123*(3), 364-369. https://doi.org/10.1016/j.geomorph.2010.08.004

Brakensiek, D. L., Osborn, H. B., & Rawls, W. J. (1979). *Field manual for research in agricultural hydrology*. Agriculture Handbook No. 224. Washington, DC: USDA.

CBPSTAC. (2013). Incorporating lag-times into the Chesapeake Bay Program. STAC Publ. No. 13-004. Edgewater, MD: Chesapeake Bay Program Scientific and Technical Advisory Committee.

Chapman, J. M., Proulx, C. L., Veilleux, M. A. N., Levert, C., Bliss, S., André, M.-E., ... Cooke, S. J. (2014). Clear as mud: A meta-analysis on the effects of sedimentation on freshwater fish and the effectiveness of sediment-control measures. *Water Res., 56*, 190-202. https://doi.org/10.1016/j.watres.2014.02.047

Characklis, G. W., Dilts, M. J., Simmons, O. D. I., Likirdopulos, C. A., Krometis, L.-A. H., & Sobsey, M. D. (2005). Microbial partitioning to settleable particles in stormwater. *Water Res., 39*(9), 1773-1782. https://doi.org/10.1016/j.watres.2005.03.004

CILAS. (2014). *Particle size analyzer user manual*. NT-1061083-41. La Source, France: CILAS.

Cole, J. J., Prairie, Y. T., Caraco, N. F., McDowell, W. H., Tranvik, L. J., Striegl, R. G., ... Melack, J. (2007). Plumbing the global carbon cycle: Integrating inland waters into the terrestrial carbon budget. *Ecosystems, 10*(1), 172-185. https://doi.org/10.1007/s10021-006-9013-8

Department of the Army. (1999). *Materials testing*. FM 5-472, NAVFAC, MO 330, AFJMAN 32-1221(I). Washington, DC: Department of the Army.

Doyle, M. W., & Ensign, S. H. (2009). Alternative reference frames in river system science. *BioScience, 59*(6), 499-510. https://doi.org/10.1525/bio.2009.59.6.8

Drummond, J. D., Davies-Colley, R. J., Stott, R., Sukias, J. P., Nagels, J. W., Sharp, A., & Packman, A. I. (2015). Microbial transport, retention, and inactivation in streams: A combined experimental and stochastic modeling approach. *Environ. Sci. Tech., 49*(13), 7825-7833. https://doi.org/10.1021/acs.est.5b01414

Drummond, J. D., Larsen, L. G., González-Pinzón, R., Packman, A. I., & Harvey, J. W. (2017). Fine particle retention within stream storage areas at base flow and in response to a storm event. *Water Resour. Res., 53*(7), 5690-5705. https://doi.org/10.1002/2016WR020202

Drummond, J., Wright-Stow, A., Franklin, P., Quinn, J., & Packman, A. (2020). Fine particle transport dynamics in response to wood additions in a small agricultural stream. *Hydrol. Proc., 34*(21), 4128-4138. https://doi.org/10.1002/hyp.13874

Edwards, K. E., & Glysson, G. D. (1999). Chapter C2: Field methods for measurement of fluvial sediment. In *Techniques of water-resources investigations reports: Book 3, Applications of hydraulics.* Reston, VA: U.S. Geological Survey.

Ferguson, R. I., Sharma, B. P., Hodge, R. A., Hardy, R. J., & Warburton, J. (2017). Bed load tracer mobility in a mixed bedrock/alluvial channel. *JGR Earth Surf., 122*(4), 807-822. https://doi.org/10.1002/2016JF003946

Foley, M. M., Bellmore, J. R., O'Connor, J. E., Duda, J. J., East, A. E., Grant, G. E., ... Wilcox, A. C. (2017). Dam removal: Listening in. *Water Resour. Res., 53*(7), 5229-5246. https://doi.org/10.1002/2017WR020457

Gao, P. (2008). Understanding watershed suspended sediment transport. *Prog. Phys.Geogr., 32*(3), 243-263. https://doi.org/10.1177/0309133308094849

Govenor, H., Krometis, L. A., & Hession, W. C. (2017). Invertebrate-based water quality impairments and associated stressors identified through the U.S. Clean Water Act. *Environ. Mgmt., 60*(4), 598-614. https://doi.org/10.1007/s00267-017-0907-3

Guida, M., Siciliano, A., & Pagano, G. (2017). Rare earth element toxicity to marine and freshwater algae. In *Rare earth elements in human and environmental health: At the crossroads between toxicity and safety* (pp. 143-153). Singapore: Pan Stanford Publishing.

Guzmán, G., Quinton, J. N., Nearing, M. A., Mabit, L., & Gómez, J. A. (2013). Sediment tracers in water erosion studies: Current approaches and challenges. *J. Soils Sed., 13*(4), 816-833. https://doi.org/10.1007/s11368-013-0659-5

Habersack, H., Kreisler, A., Rindler, R., Aigner, J., Seitz, H., Liedermann, M., & Laronne, J. B. (2017). Integrated automatic and continuous bedload monitoring in gravel bed rivers. *Geomorphology, 291*, 80-93. https://doi.org/10.1016/j.geomorph.2016.10.020

Haddadchi, A., Ryder, D. S., Evrard, O., & Olley, J. (2013). Sediment fingerprinting in fluvial systems: Review of tracers, sediment sources, and mixing models. *Intl. J. Sed. Res., 28*(4), 560-578. https://doi.org/10.1016/S1001-6279(14)60013-5

Hamilton, S. K. (2012). Biogeochemical time lags may delay responses of streams to ecological restoration. *Freshwater Biol., 57*(S1), 43-57. https://doi.org/10.1111/j.1365-2427.2011.02685.x

Harvey, J. W., Drummond, J. D., Martin, R. L., McPhillips, L. E., Packman, A. I., Jerolmack, D. J., ... Tobias, C. R. (2012). Hydrogeomorphology of the hyporheic zone: Stream solute and fine particle interactions with a dynamic streambed. *J. Geophys. Res., 117*(G4), article G00N11. https://doi.org/10.1029/2012JG002043

Keaton, J. N., Messinger, T., & Doheny, E. J. (2005). Development and analysis of regional curves for streams in the non-urban valley and ridge physiographic province, Maryland, Virginia, and West Virginia. USGS Scientific Investigations Report. 2005-5076. Reston, VA: U.S. Geological Survey. https://doi.org/10.3133/sir20055076

Keys, T. A., Govenor, H., Jones, C. N., Hession, W. C., Hester, E. T., & Scott, D. T. (2018). Effects of large wood on floodplain connectivity in a headwater Mid-Atlantic stream. *Ecol. Eng., 118*, 134-142. https://doi.org/10.1016/j.ecoleng.2018.05.007

Keys, T. A., Jones, C. N., Scott, D. T., & Chuquin, D. (2016). A cost-effective image processing approach for analyzing the ecohydrology of river corridors. *Limnol. Oceanog. Methods, 14*(6), 359-369. https://doi.org/10.1002/lom3.10095

Kreider, T. A. (2012). Rare earth elements as a tracer to understand sediment fate and transport in small streams. MS thesis. Blacksburg, VA: Virginia Tech, Department of Biological Systems Engineering.

Larsen, L. G., & Harvey, J. W. (2017). Disrupted carbon cycling in restored and unrestored urban streams: Critical timescales and controls. *Limnol. Oceanog., 62*(S1), S160-S182. https://doi.org/10.1002/lno.10613

Larsen, M. C., Gellis, A. C., Glysson, G. D., Gray, J. R., & Horowitz, A. J. (2010). Fluvial sediment in the environment: A national challenge. *Proc. Joint Fed. Interagency Conf: Hydrology and Sedimentation for a Changing Future: Existing*

and Emerging Issues (p. 14). Reston, VA: U.S. Geological Survey.
Maaß, A., & Schüttrumpf, H. (2019). Elevated floodplains and net channel incision as a result of the construction and removal of water mills. *Geografiska Annaler: Series A, Phys. Geogr., 101*(2), 157-176. https://doi.org/10.1080/04353676.2019.1574209
Mahler, B. J., Bennett, P. C., & Zimmerman, M. (1998). Lanthanide-labeled clay: A new method for tracing sediment transport in karst. *Groundwater, 36*(5), 835-843. https://doi.org/10.1111/j.1745-6584.1998.tb02202.x
Mao, L., Dell'Agnese, A., & Comiti, F. (2017). Sediment motion and velocity in a glacier-fed stream. *Geomorphology, 291*, 69-79. https://doi.org/10.1016/j.geomorph.2016.09.008
Martin-Ortega, J., Glenk, K., & Byg, A. (2017). How to make complexity look simple? Conveying ecosystems restoration complexity for socio-economic research and public engagement. *PLoS One, 12*(7), e0181686. https://doi.org/10.1371/journal.pone.0181686
Meals, D. W., Dressing, S. A., & Davenport, T. E. (2010). Lag time in water quality response to best management practices: A review. *J. Environ. Qual., 39*(1), 85-96. https://doi.org/10.2134/jeq2009.0108
Michaelides, K., Ibraim, I., Nord, G., & Esteves, M. (2010). Tracing sediment redistribution across a break in slope using rare earth elements. *Earth Surf. Proc. Landforms, 35*(5), 575-587. https://doi.org/10.1002/esp.1956
Miller, J. R., Mackin, G., & Miller, S. M. (2015). *Application of geochemical tracers to fluvial sediment.* New York, NY: Springer. https://doi.org/10.1007/978-3-319-13221-1
Muirhead, R. W., Davies-Colley, R. J., Donnison, A. M., & Nagels, J. W. (2004). Faecal bacteria yields in artificial flood events: Quantifying in-stream stores. *Water Res., 38*(5), 1215-1224. https://doi.org/10.1016/j.watres.2003.12.010
Naden, P. S. (2010). The fine-sediment cascade. In *Sediment cascades an integrated approach* (1st Ed., pp. 271-305). Hoboken, NJ: Wiley-Blackwell. https://doi.org/10.1002/9780470682876.ch10
NRCS. (2017). Web soil survey. Washington, DC: USDA Natural Resources Conservation Service. Retrieved from https://websoilsurvey.sc.egov.usda.gov
Owens, P. N. (2008). Sediment behaviour, functions, and management in river basins. In P. N. Owens (Ed.), *Sustainable management of sediment resources, sediment management at the river basin scale* (Vol. 4, pp. 1-30). Amsterdam: Elsevier. https://doi.org/10.1016/S1872-1990(08)80003-7
Owens, P. N., Batalla, R. J., Collins, A. J., Gomez, B., Hicks, D. M., Horowitz, A. J., ... Trustrum, N. A. (2005). Fine-grained sediment in river systems: Environmental significance and management issues. *River Res. Appl., 21*(7), 693-717. https://doi.org/10.1002/rra.878
Phillips, J. M., Russell, M. A., & Walling, D. E. (2000). Time-integrated sampling of fluvial suspended sediment: A simple methodology for small catchments. *Hydrol. Proc., 14*(14), 2589-2602. https://doi.org/10.1002/1099-1085(20001015)14:14<2589::AID-HYP94>3.0.CO;2-D
Pizzuto, J. E. (2014). Long-term storage and transport length scale of fine sediment: Analysis of a mercury release into a river. *Geophys. Res. Letters, 41*(16), 5875-5882. https://doi.org/10.1002/2014GL060722
Pizzuto, J., Schenk, E. R., Hupp, C. R., Gellis, A., Noe, G., Williamson, E., ... Newbold, D. (2014). Characteristic length scales and time-averaged transport velocities of suspended sediment in the Mid-Atlantic region, USA. *Water Resour. Res., 50*(2), 790-805. https://doi.org/10.1002/2013WR014485
Polyakov, V. O., & Nearing, M. A. (2004). Rare earth element oxides for tracing sediment movement. *Catena, 55*(3), 255-276. https://doi.org/10.1016/S0341-8162(03)00159-0
Polyakov, V. O., Kimoto, A., Nearing, M. A., & Nichols, M. H. (2009). Tracing sediment movement on a semiarid watershed using rare earth elements. *SSSA J., 73*(5), 1559-1565. https://doi.org/10.2136/sssaj2008.0378
Quinlan, E., Gibbins, C. N., Batalla, R. J., & Vericat, D. (2015). Impacts of small-scale flow regulation on sediment dynamics in an ecologically important upland river. *Environ. Mgmt., 55*(3), 671-686. https://doi.org/10.1007/s00267-014-0423-7
Spencer, K. L., Droppo, I. G., He, C., Grapentine, L., & Exall, K. (2011). A novel tracer technique for the assessment of fine sediment dynamics in urban water management systems. *Water Res., 45*(8), 2595-2606. https://doi.org/10.1016/j.watres.2011.02.012
Thompson, T. W., Hession, C. W., & Scott, D. (2012). StREAM lab at Virginia Tech. *Resource, 19*(2), 8-9. St. Joseph, MI: ASABE.
USEPA. (1998). Method 6020A: Inductively coupled plasma - mass spectrometry. Revision 1. Washington, DC: U.S. Environmental Protection Agency.
USEPA. (1999). Protocol for developing sediment TMDLs. EPA 841-B-99-004. Washington, DC: U.S. Environmental Protection Agency.
USEPA. (2007). Method 3051A: Microwave-assisted acid digestion of sediments, sludges, soils, and oils. Revision 1. Washington, DC: U.S. Environmental Protection Agency.
USEPA. (2016). Assessment and total maximum daily load tracking and implementation system (ATTAINS). Washington, DC: Environmental Protection Agency. Retrieved from http://www2.epa.gov/waterdata/assessment-and-total-maximum-daily-load-tracking-and-implementation-system-attains
USGS. (2002). Rare earth elements: Critical resources for high technology. Fact Sheet 087-02. Reston, VA: U.S. Geological Survey. Retrieved from pubs.usgs.gov/fs/2002/fs087-02/fs087-02.pdf
Van Meter, K. J., Van Cappellen, P., & Basu, N. B. (2018). Legacy nitrogen may prevent achievement of water quality goals in the Gulf of Mexico. *Science, 360*(6387), 427-430. https://doi.org/10.1126/science.aar4462
Von Bertrab, M. G., Krein, A., Stendera, S., Thielen, F., & Hering, D. (2013). Is fine sediment deposition a main driver for the composition of benthic macroinvertebrate assemblages? *Ecol. Indic., 24*, 589-598. https://doi.org/10.1016/j.ecolind.2012.08.001
Waters, T. F. (1995). Sediment in streams: Sources, biological effects, and control. Monograph 7. Bethesda, MD: American Fisheries Society.
Wood, P. J., & Armitage, P. D. (1997). Biological effects of fine sediment in the lotic environment. *Environ. Mgmt., 21*(2), 203-217. https://doi.org/10.1007/s002679900019
Zhang, Q., Ball, W. P., & Moyer, D. L. (2016). Decadal-scale export of nitrogen, phosphorus, and sediment from the Susquehanna River basin, USA: Analysis and synthesis of temporal and spatial patterns. *Sci. Total Environ., 563-564*, 1016-1029. https://doi.org/10.1016/j.scitotenv.2016.03.104
Zhang, X. C. C., Friedrich, J. M. M., Nearing, M. A. A., & Norton, L. D. D. (2001). Potential use of rare earth oxides as tracers for soil erosion and aggregation studies. *SSSA J., 65*(5), 1508-1515. https://doi.org/10.2136/sssaj2001.6551508x